

# ***BARX2* expression is downregulated by CpG island hypermethylation and is associated with suppressed cell proliferation and invasion of gastric cancer cells**

JUAN MA<sup>1\*</sup>, LING-LING XIA<sup>2\*</sup>, XUE-QING YAO<sup>3</sup>, SHI-MIN ZHENG<sup>1</sup>,  
SHI LI<sup>2</sup>, LI-SHU XU<sup>1</sup>, WEI-HONG SHA<sup>1</sup> and ZE-SONG LI<sup>2</sup>

<sup>1</sup>Department of Gastroenterology and Hepatology, Guangdong Provincial People's Hospital, Guangdong Academy of Medical Sciences, and Guangdong Provincial Geriatrics Institute, Guangzhou, Guangdong 510080; <sup>2</sup>Guangdong Key Laboratory of Systems Biology and Synthetic Biology for Urogenital Tumors, Shenzhen Second People's Hospital, First Affiliated Hospital of Shenzhen University, Shenzhen, Guangdong 518000; <sup>3</sup>Department of General Surgery, Guangdong Provincial People's Hospital, Guangdong Academy of Medical Sciences, Guangzhou, Guangdong 510080, P.R. China

Received July 26, 2019; Accepted February 21, 2020

DOI: 10.3892/or.2020.7558

**Abstract.** BarH-like homeobox 2 (*BARX2*), a homeobox gene, is associated with several types of cancers. The present study aimed to determine whether DNA methylation downregulates *BARX2* expression and whether *BARX2* is associated with suppression of gastric carcinogenesis. *BARX2* protein expression in normal and cancerous gastric tissues and various gastric cancer (GC) cell lines was detected using immunohistochemical and western blot assays. *BARX2* mRNA levels were detected using both reverse transcription-polymerase chain reaction (RT-PCR) and quantitative PCR (qPCR). Promoter hypermethylation in GC cells was detected using methylation-specific PCR or bisulfite DNA sequencing PCR. Effects of *BARX2* expression on GC cell proliferation, clonal formation, and migration were evaluated after lentivirus-*BARX2* transfection. The effect of stable *BARX2* transfection on tumor formation

was assessed in a nude xenograft mouse model. *BARX2* was strongly expressed in the normal gastric mucosa, but weakly or not expressed in GC tissues and most GC cell lines. *BARX2* expression was negatively correlated with DNMT (a marker for DNA methylation) expression in the gastric tissues. The *BARX2* promoter fragment was hypermethylated in the GC cell lines. Overexpression of *BARX2* significantly inhibited GC cell proliferation, clonal formation, and migration. Stable *BARX2* transfection inhibited tumor formation in xenograft mice, which was correlated with decreased expression of E-cadherin, proliferation markers, and matrix metalloproteinases. In conclusion, *BARX2* expression is aberrantly reduced in GC, which is associated with increased DNA methylation of its promoter. *BARX2* inhibits GC cell proliferation, migration, and tumor formation, suggesting that *BARX2* acts as a tumor suppressor in gastric carcinogenesis.

---

*Correspondence to:* Dr Ze-Song Li, Guangdong Key Laboratory of Systems Biology and Synthetic Biology for Urogenital Tumors, Shenzhen Second People's Hospital, First Affiliated Hospital of Shenzhen University, 3002 Sungang West Road, Futian, Shenzhen, Guangdong 518000, P.R. China  
E-mail: lzssc@yahoo.com

Dr Wei-Hong Sha, Department of Gastroenterology and Hepatology, Guangdong Provincial People's Hospital, Guangdong Academy of Medical Sciences, and Guangdong Provincial Geriatrics Institute, 106 Zhongshan 2nd Road, Yuexiu, Guangzhou, Guangdong 510080, P.R. China  
E-mail: shawei hong@gdph.org.cn

\*Contributed equally

**Key words:** *BARX2*, DNA methylation, proliferation, invasion, gastric cancer

## **Introduction**

Globally, gastric cancer (GC) is the fifth most commonly diagnosed cancer and the third leading cause of cancer-related mortality (1,2). Although the incidence and mortality of GC in China are declining, GC still ranks second in both incidence and mortality, with an estimated 679,100 new cases and 498,000 deaths reported in 2015 (3). The high mortality is largely due to the late diagnosis of the disease; at present, the majority of newly diagnosed cases have locally advanced or metastatic disease. Therefore, identification of factors that participate in the development and progression of GC will help establish optimal prevention, early diagnosis, and treatment strategies for GC.

Homeobox genes, which encode homeodomain transcription factors, have been demonstrated to play critical roles in embryo patterning along the anterior-posterior axis and maintaining patterns in adult tissues (4,5). Studies have demonstrated that some homeobox genes are upregulated whereas others are downregulated in cancers, and some homeobox

genes exhibit both tumor-promoting and tumor-suppressing activities depending on the specificity of the tissues and cells (6-9).

*BARX2*, also known as BarH-like homeobox 2, is located at 11q24-q25 and encodes a 254-amino acid homeodomain transcription factor (10). *BARX2* plays a key role during embryonic development (11,12) and participates in cytoskeletal organization, growth factor signaling, cell adhesion, and transcriptional regulation (11,13-15). Several studies have shown that *BARX2* downregulation is associated with ovarian cancer, breast cancer, primary hepatocellular carcinoma (HCC), colorectal cancer, lung cancer, and GC (16), along with poor patient prognosis (16-21). In addition, *BARX2* promotes myogenic differentiation, regulates muscle-specific gene expression, and regulates cell adhesion and cytoskeleton remodeling during muscle cell fusion and cartilage formation (10). *BARX2* regulates various cellular adhesion molecules and promotes tissue differentiation (14). Moreover, *BARX2* functions as a tumor suppressor, with anti-oncogenic effects, as shown in an *in vitro* study (16). However, the underlying mechanisms by which *BARX2* expression is downregulated and by which *BARX2* exerts anti-oncogenic effects remain to be elucidated.

Several mechanisms, such as loss of heterozygosity, histone deacetylation, gene amplification, and especially CpG island promoter hypermethylation are involved in the aberrant expression of homeobox genes (22-24). DNA methylation within the promoter of tumor-suppressor genes, which is commonly found in cancer cells, leads to transcriptional silencing, and subsequently promotes cancer development (25). DNA methyltransferase (DNMT) is responsible for DNA methylation (26). Promoter hypermethylation and decreased expression of various homeobox genes, such as *CDX1* (22), *CDX2* (23) and *PDX1* (24), have been reported in cancers such as squamous esophageal cancer, GC, and colorectal cancers. Whether CpG island promoter hypermethylation is responsible for the downregulation or loss of *BARX2* expression is unclear. Therefore, the present study aimed to determine whether DNA methylation downregulates *BARX2* expression and whether *BARX2* is associated with suppression of gastric carcinogenesis.

## Materials and methods

**Tissue microarray chips, cell lines, and animals.** The tissue microarray chips containing formalin-fixed, paraffin-embedded specimens surgically taken from gastric malignancies of 208 patients and endoscopically taken from normal gastric mucosa of 8 individuals were provided by Xi'an Alena Biotechnology Company (Xi'an, China) and used for immunohistochemical *BARX2* detection. The clinical and histological characteristics of the patients and normal controls are listed in Table I.

To observe the correlation between the expression of *BARX2* and DNMT-1 (a commonly used marker of DNA methylation), a separate batch of tissue microarray chips containing specimens from 22 cases of gastric adenocarcinoma and 8 normal controls were used for immunohistochemical detection of *BARX2* and DNMT-1.

Human GC cell lines including AGS, MGC803 (both derived from primary human gastric adenocarcinoma),

MKN7 (metastatic gastric tubular adenocarcinoma), MKN74 (metastatic gastric tubular adenocarcinoma), and HGC27 (metastatic gastric carcinoma) were purchased from the Type Culture Collection of the Chinese Academy of Sciences (Shanghai, China). GES1 (a normal gastric mucosal cell) was kindly provided by Dr Sui Peng (The First Affiliated Hospital, Sun Yat-sen University, Guangzhou, China). Cells were grown in F-12K nutrient mixture containing 10% fetal bovine serum (FBS; Gibco; Thermo Fisher Scientific, Inc.) in a cell culture incubator with 5% CO<sub>2</sub> at 37°C for more than 24 h, and then lysed with 0.05% of trypsin-EDTA (Thermo Fisher Scientific, Inc.). All cell lines were used for reverse transcription polymerase chain reaction (RT-PCR) or real-time quantitative PCR (qPCR), and AGS cells were used for western blot analysis, qPCR, and lentivirus (LV) transfection.

Ten male BALB/c-nu/nu mice (weighing 16-18 g) were provided by Guangdong Medical Laboratory Animal Center (Guangzhou, China) and used to determine the effect of *BARX2* on tumorigenicity. Mice were housed at room temperature with 40-60% humidity, and with a light cycle of 10-h light/14-h dark under pathogen-free conditions. All animal protocols were approved by the Guangdong General Hospital Ethics Committee.

**Immunohistochemical staining.** After deparaffinizing and rehydration, the chips were incubated with mouse anti-*BARX2* (dilution 1:50; cat. no. sc-53177; Santa Cruz Biotechnology) and rabbit anti-DNMT-1 (dilution 1:50; product code ab19905; Abcam) primary antibodies overnight at 4°C. The chips were then incubated with peroxidase-conjugated anti-mouse secondary antibody (dilution 1:100; cat. no. 7076; Cell Signaling Technology) and peroxidase-conjugated anti-rabbit secondary antibody (dilution 1:100; cat. no. 7074; Cell Signaling Technology) respectively. The chips were visualized with 3,3'-diaminobenzidine (1 mg/ml) and then counterstained with hematoxylin. Finally, *BARX2* expression was analyzed using a Leica DM2500 system microscope (magnification, x100; Meyer Instruments). The percentage of the area with positively stained cells, defined as the area ratio, was determined using ImageJ 1.52a software (National Institutes of Health, Bethesda, MD, USA) (<http://imagej.net/Downloads>) to represent quantitative expression. The percentage of positively stained cells (i.e. cells with *BARX2* signal among GC cells) was also calculated.

**Western blot analysis.** AGS cells were washed with ice-cold phosphate-buffered saline (PBS; Thermo Fisher Scientific, Inc.) and scraped using a 10-cm cold plastic cell scraper. After centrifugation at 2,000 x g at 4°C for 5 min, the cell pellet was added into RIPA lysate buffer (Sigma-Aldrich; Merck KGaA) containing protease inhibitors for protein extraction. The AGS cell lysates were electrophoresed on sodium dodecyl sulfate-polyacrylamide 5% gel (SDS-PAGE) and transferred to a polyvinylidene difluoride membrane. The membrane was probed with primary antibodies against *BARX2* (dilution 1:1,000; cat. no. sc-53177; Santa Cruz Biotechnology), proliferating cell nuclear antigen (PCNA) (dilution 1:1,000; product code ab146970), Ki-67 (dilution 1:500, product code; ab254123), matrix metalloproteinase-7 (MMP7) (dilution 1:1,000; product code ab207299), MMP9 (dilution 1:2,000; product

Table I. Associations of BARX2 protein expression with demographic and pathological characteristics of the patients with gastric cancer (n=208) and normal controls (n=8).

Variable	Group	Cases (n)	BARX2 expression <sup>a</sup>	Positive percentage (%)
Age (years)	Gastric cancer patients			
	<60	103	0.469 (0.018, 1.859)	53.40 (55/103)
	60-79	98	0.171 (0.018, 2.037)	55.10 (54/98)
	≥80	7	0.017 (0.016, 2.868)	42.86 (3/7)
	Normal controls			
	<60	8	6.085 (4.032, 13.049)	100 (8/8)
Sex	Gastric cancer patients			
	Male	156	0.351 (0.018, 1.854)	51.92 (81/156)
	Female	52	0.241 (0.018, 2.631)	59.61 (31/52)
	Normal controls			
	Male	5	6.640±2.780	62.5 (5/8)
	Female	3	10.287±2.330	37.5 (3/8)
Pathological types	Normal	8	6.085 (4.032, 13.049)	100 (8/8)
	Mucinous adenocarcinoma	12	0.06 (0.018, 1.952)	41.67 (5/12)
	Signet-ring cell carcinoma	6	0.052 (0.025, 0.491)	33.33 (2/6)
	Undifferentiated carcinoma	5	0.891 (0.243, 5.463)	100 (5/5)
	Carcinoid	3	0.19 (0.021, 4.499)	0.00 (0/3)
	Malignant interstitialoma	9	0.0189 (0.016, 0.018)	100 (9/9)
	Squamous cell carcinoma	1	0.092	100 (1/1) <sup>d</sup>
TNM stage <sup>b</sup>	Normal	8	6.085 (4.032, 13.049)	100 (8/8)
	I	116	0.641 (0.018, 2.318)	59.48 (69/116)
	II	41	0.039 (0.018, 0.927)	36.59 (15/41)
	III	12	0.022 (0.017, 1.509)	41.67 (5/12)
	IV	3	0.021 (0.016, 5.867) <sup>f</sup>	33.33 (1/3) <sup>e</sup>
Pathological grading	Normal	8	6.085 (4.032, 13.049)	100.00 (8/8)
	Well-differentiated	8	0.659 (0.079, 2.825)	62.50 (5/8)
	Moderately differentiated	40	0.459 (0.017, 2.42)	47.5 (19/40)
	Poorly differentiated	110	0.444 (0.019, 2.002)	53.64 (59/110)
	Undifferentiated	8	0.143 (0.016, 1.758) <sup>e</sup>	50 (4/8)
	Not reported <sup>c</sup>	5	0.039 (0.018, 9.03)	40 (2/5)
Lymph node metastasis	No	150	0.426 (0.019, 2.028)	54.67 (82/150)
	Yes	24	0.02 (0.017, 1.174)	36.36 (8/22)

<sup>a</sup>Area ratio, median (upper quartile, lower quartile). <sup>b</sup>Gastric adenocarcinoma only, with eight normal controls. <sup>c</sup>Excluded from the analysis. <sup>d</sup>P<0.05, <sup>e</sup>P<0.01 and <sup>f</sup>P<0.001. BARX2, BarH-like homeobox 2.

code ab73734; all from Abcam), E-cadherin (dilution 1:1,000; cat. no. 3195) and MMP3 (dilution 1:1,000; cat. no. 14351; both from Cell Signaling Technology), and subsequently with horse-radish peroxidase-conjugated secondary antibodies (dilution 1:2,500; cat. no. BA1055; Boster Biological Technology, Ltd.).  $\beta$ -actin (dilution 1:1500; Abcam) served as an internal control. An enhanced chemiluminescence system (Amersham) was used to visualize the antigen-antibody complex. The ImageJ 1.52a software (National Institutes of Health) was used for quantification.

**Total RNA extraction, RT-PCR and qPCR.** Total RNA was extracted using TRIzol reagent (Invitrogen; Thermo Fisher Scientific, Inc.) after the cells were harvested. RNA

concentrations were measured using a NanoDrop 2000/2000c spectrophotometer (Thermo Fisher Scientific, Inc.). RNA was reverse transcribed to complementary DNA using the PrimeScript™ RT reagent Kit (Perfect Real Time; Takara Bio Inc.). The PCR program was performed in a 20- $\mu$ l reaction mixture containing 2  $\mu$ l complementary DNA and 0.2 U Hot Start *Taq* DNA polymerase (cat. no. M0495S; New England Biolabs, Inc.) and run for 30 cycles of denaturation (at 94°C for 30 sec), annealing (at 56°C for 30 sec) and elongation (at 72°C for 45 sec). The primer sequences for RT-PCR are shown in Table II. Glyceraldehyde-3-phosphate dehydrogenase (GAPDH) was used as the internal control.

AGS cells were used for qPCR using the ABI PRISM 7000 Fluorescent Quantitative PCR System (Applied Biosystems;

Table II. Primer sequences for *BARX2* mRNA expression, MSP and BSP analysis.

Gene	Primer sequence	Product size (bp)
<i>BARX2</i> (RT-PCR)	Forward: 5'-GCAGCGAGTCAGAGACGGAACA-3' Reverse: 5'-GCCATCTCTAAGGGGACATCACG-3'	424
<i>GAPDH</i> (RT-PCR)	Forward: 5'-GTCAACGGATTTGGTCGTATTG-3' Reverse: 5'-CTCCTGGAAGATGGTGATGGG-3'	200
<i>BARX2</i> (qPCR)	Forward: 5'-CGGAGTCGCACCATCTTCAC-3' Reverse: 5'-GAGCCAAGTCCAACCTGTCT-3'	100
$\beta$ -actin (qPCR)	Forward: 5'-GGCACCACACCTTCTACAATGAG-3' Reverse: 5'-GGATAGCACAGCCTGGATAGCA-3'	167
MSP	Forward: 5'-AAGAGTAATGTAAAGTCGGGGTTTCGA-3' Reverse: 5'-ACCGCCAATAAACTAAATACTTACGAACG-3'	208
USP	Forward: 5'-AAGAGTAATGTAAAGTTGGGGTTTTGA-3' Reverse: 5'-CCACCAATAAACTAAATACTTACAAACAAT-3'	267
BSP	Forward: 5'-GGGGAGGGGGAGGAGATTAATA-3' Reverse: 5'-AAACCCACCCRCAAATCAACATCTTC-3'	267

*BARX2*, BarH-like homeobox 2; MSP, methylation-specific PCR analysis; USP, unmethylation-specific PCR analysis; BSP, bisulfite DNA sequencing PCR analysis.

Thermo Fisher Scientific, Inc.). The PCR program was carried out in a 20  $\mu$ l mixture containing the Power SYBR Green PCR Master Mix (Applied Biosystems; Thermo Fisher Scientific, Inc.), 500 nmol of the primers and 300 ng of complementary DNA templates. An initial denaturation at 95°C for 5 min was followed by 50 cycles of denaturation (at 94°C for 20 sec), annealing (at 60°C for 20 sec), and elongation (at 72°C for 40 sec), with a final extension at 72°C for 5 min. The melting curves and the generated Ct values, which were calculated using the  $\Delta\Delta C_q$ -method and expressed as  $2^{-\Delta\Delta C_q}$  (27), were used to quantify *BARX2* mRNA. The primer sequences for RT-qPCR are shown in Table II.

**Methylation-specific PCR (MSP) and bisulfite DNA sequencing PCR (BSP).** The TRED database (28) and Methprimer software (29) were used to search a 1,000-bp genomic sequence that included the ATG translation starting codon (-1,000 nt to 0 nt) of *BARX2* to predict the promoter. MSP and BSP were used to examine the methylation status of the CpG islands in the five GC cell lines.

First, DNA was isolated from the cells using the DNeasy Blood and Tissue Kit (Qiagen China Co. Ltd.). Each genomic DNA sample (1.0  $\mu$ g) was denatured with NaOH (2 mol/l) at 37°C for 10 min, and incubated with sodium bisulfate (3 mol/l, pH 5.0; Sigma-Aldrich; Merck KGaA) at 50°C for 16 h. The bisulfite-treated DNA was amplified with methylation-specific or unmethylation-specific primers (Table II). For MSP analysis, the PCR program was carried out in a 25- $\mu$ l reaction mixture containing 10 pmol/l primers, 25  $\mu$ mol/l deoxynucleoside triphosphates, 2  $\mu$ l of bisulfate-treated DNA, and 0.5 U of Hot-Start *Taq* polymerase. The hot start at 95°C for 20 min was followed by 40 cycles of denaturation (at 94°C for 30 sec), annealing (at 52°C for 30 sec), and elongation (at 72°C for 45 sec), with a final extension at 72°C for 10 min. The PCR products were visualized on a 2% agarose gel and stained with ethidium bromide.

For BSP analysis, the bisulfite-treated DNA sample (2  $\mu$ l) was amplified in 20  $\mu$ l reaction mixture, using the same PCR program for MSP, except that the primers used were the bisulfate-treated DNA sequencing PCR primers (Table II). For GC cell lines, the fragment containing 27 CpG sites, as identified by the Methprimer software, was amplified using bisulfite-modified DNA as a template and inserted into the *pGEM-T4* vector after purification (Promega). Ten white clones were selected for each sample and were then sequenced to determine the aberrant methylation of each CpG site of the wild-type and modified sequences of the *BARX2* promoter fragment in MGC803, MKN74 and HGC27 cells.

**Lentiviral (LV) transfection of AGS cells.** LV specifically targeting *BARX2* for gene overexpression and sequences of the controls were purchased from Biolink Biotechnology Co. (Shanghai, China). *LV-BARX2* or *LV-empty* vectors were transfected into AGS cells following the manufacturer's protocol. Puromycin (5  $\mu$ g/ml) was used for 1 week to eradicate untransfected cells, and then the transfected cells (AGS-LV-*BARX2* and AGS-LV cells) were passaged at a ratio of 1:15 (vol/vol), and cultured for 4 weeks in F-12K nutrient mixture containing puromycin (5  $\mu$ g/ml). Finally, stably transfected clones were selected for immunohistochemical detection of *BARX2* expression and maintained in the F-12K nutrient mixture prior to the subsequent experiments.

**Cell proliferation assays.** Cell proliferation was detected using the Cell Counting Kit-8 (CCK-8, Dojindo Laboratories). Briefly, AGS cells transfected with *LV-BARX2* or *LV-empty* were seeded into 96-well plates at  $2.0 \times 10^3$  or  $4.0 \times 10^3$  cells per well. The relative ratio of absorbance at 490 nm of the transfected cells (i.e. AGS-*BARX2* and AGS-LV cells) was recorded with a microplate reader (Bio-Rad Laboratories, Inc.) at 24, 48, 72 and 96 h, and expressed as a proliferation index. Each experiment was performed in quadruplicate.

Cell proliferation was also detected using 5'-ethynyl-2'-deoxyuridine (EdU) (ThermoFisher Scientific, Inc.). Briefly, the transfected cells were seeded into 12-well-plates at  $4.0 \times 10^5$  cells per well, stained with EdU and 4',6-diamidino-2-phenylindole (DAPI) (Thermo Fisher Scientific, Inc.) 48 h later, and randomly photographed under four high-power fields with a fluorescence microscope.

**Colony formation assay.** Transfected cells were seeded into 6-well plates at three different cell densities ( $0.5 \times 10^3$ ,  $1.0 \times 10^3$  and  $2.0 \times 10^3$  cells per well) and cultured for 4 weeks. Cell colonies were fixed with methyl alcohol for 15 min and stained with 0.1% crystal violet solution for 15 min and were then counted under the Leica DM2500 system microscope (magnification, x40; Meyer Instruments). Three independent experiments were performed, each in triplicate.

**Cell migration assay.** Cell migration was assayed using the Transwell 24-well Boyden chamber with a 8- $\mu$ m polycarbonate membrane (Corning, Inc.). Briefly,  $3.0 \times 10^4$  cells were plated in the upper chamber containing 200  $\mu$ l serum-free media, while the bottom chamber contained 500  $\mu$ l media supplemented with 10% FBS as a chemoattractant. After 48 h, the migrated cells were fixed by 4% paraformaldehyde, stained with 0.1% crystal violet, and finally eluted with 1 ml of 33% acetic acid. Absorbance of the migrated cells was measured at 460 nm and expressed as an A460 value. Three independent experiments were performed.

**Tumorigenicity in nude mice.** Ten male BALB/c-nu/nu mice were divided into two groups (n=5 per group). The monoclonal LV-BARX2 or LV-empty transfectants of AGS cells (*i.e.* AGS cells stably transfected with LV-BARX2 or LV-empty vectors,  $1.0 \times 10^7$  cells in 150  $\mu$ l PBS) were inoculated subcutaneously into the right flank of the mice. Tumor formation was observed for 4 weeks, and then the mice were euthanized. The xenografted tumors were dissected and the volume (V) was calculated according to the following formula:  $V (\text{mm}^3) = \text{length} (\text{mm}) \times \text{width}^2 (\text{mm}^2)$ . Whole proteins were extracted to detect Ki-67, PCNA, E-cadherin, and MMPs using western blot analysis as described above.

**Statistical analysis.** Numerical data are expressed as mean  $\pm$  standard error of the mean (SEM) or median (25, 75%). The Student's t-test was used for numeric data with normal distribution, and the Mann-Whitney U-test was used for numeric data with abnormal distribution. The Chi-square or Fisher's exact test, where appropriate, was used for categorical data, with odds ratio (OR) and 95% confidence interval (CI). Correlation was performed using Pearson linear correlation. All statistical analyses were performed using SPSS 16.0 software (SPSS, Inc.). A P-value of  $<0.05$  was assigned as indicative of statistical significance.

## Results

**BARX2 expression is downregulated in GC tissues and cell lines.** Immunohistochemical analysis showed that BARX2 was expressed in the nuclei and cytoplasm of glandular epithelial cells in the normal gastric tissues (Fig. 1A<sub>g</sub> and H). In

contrast, BARX2 expression was low or even undetectable in the gastric malignant tissues (Fig. 1A<sub>a-f</sub>). BARX2 was expressed in all 8 (100%) normal gastric mucosal samples, and 112 (53.85%) cases with gastric malignancy ( $\chi^2=4.163$ ,  $P=0.041$ ). Quantitative analysis showed that the positive staining area was significantly larger in the normal group (n=8) compared to the gastric malignant group (n=208,  $8.01 \pm 1.95$  vs.  $1.29 \pm 0.14$ ,  $P<0.001$ ) (Fig. 1B); the area was significantly larger in the normal group than in the subgroup with gastric adenocarcinoma (n=172,  $8.01 \pm 1.95$ , vs.  $1.23 \pm 0.14$ ,  $P<0.001$ ). BARX2 mRNA levels were also low in AGS, MKN74, and MKN7 cells, MGC803 and HGC27 cells compared to GES1, as detected by qPCR (vs. GES1,  $P<0.001$ ) (Fig. 1C).

The associations of BARX2 expression with demographic, clinical, and pathological characteristics are summarized in Table I. There was a significant difference in the positive percentage of BARX2 ( $\chi^2=4.748$ ,  $P=0.029$ ), but not in the area ratio, among the different pathological types of gastric malignant tumors. As most patients had gastric adenocarcinoma, we further investigated the associations between BARX2 expression with pathological TNM stages and grading of gastric adenocarcinoma (Table I). BARX2 protein expression was positive in normal gastric tissues (Fig. 2A), but began to decline in gastric adenocarcinoma from TNM stage I to IV (Fig. 2B-G) in terms of both percentage and area ratio (Table I,  $\chi^2=22.496$ ,  $P<0.001$ ). Additionally, there was a gradual decline among the different pathological grades of differentiation (well-differentiated, moderately differentiated, poorly differentiated, and undifferentiated) in terms of the percentage and area ratio ( $\chi^2=18.255$ ,  $P=0.001$ ) (Table I).

**BARX2 expression is negatively correlated with DNMT-1 expression.** BARX2 expression was commonly present in normal gastric mucosal glands, while DNMT-1 expression was often positive in gastric adenocarcinoma cells (Fig. 3A). The quantitative protein expression of BARX2 in gastric adenocarcinoma was lower than that of the normal mucosa [0.05 (0.021, 2.121) vs. 7.67 (4.657, 13.282),  $P=0.001$ ], whereas the expression pattern of DNMT-1 was reversed [0.018 (0.016, 0.166) (control) vs. 3.3395 (1.312, 6.007) (adenocarcinoma),  $P<0.001$ ] (Fig. 3B). BARX2 expression was negatively correlated with DNMT-1 expression (Pearson correlation  $r=-0.369$ ,  $P=0.045$ ) (Fig. 3C).

**BARX2 promoter is hypermethylated in GC cell lines.** Locations of two putative CpG islands were identified using the Methprimer software (Fig. 4A). The methylation status of these CpG islands was determined using MSP and BSP analyses in the five GC cell lines. MSP showed partial methylation of BARX2 in MGC803, MKN7, MKN74, and AGS cells and complete methylation in HGC27 cells (Fig. 4B). BSP analysis demonstrated 27 candidate CpG sites for methylation in the BARX2 promoter fragment as none of these sites was altered into T (Fig. 4C). Among the cell lines studied, MGC803 cells displayed a high level of methylation in most of the 27 CpG sites, while MKN74 and HGC27 cells only showed partial methylation of the 27th CpG site (Fig. 4D). Both MSP and BSP showed that DNA hypermethylation was present at the 5'flanking conserved promoter region of BARX2 in GC cells.

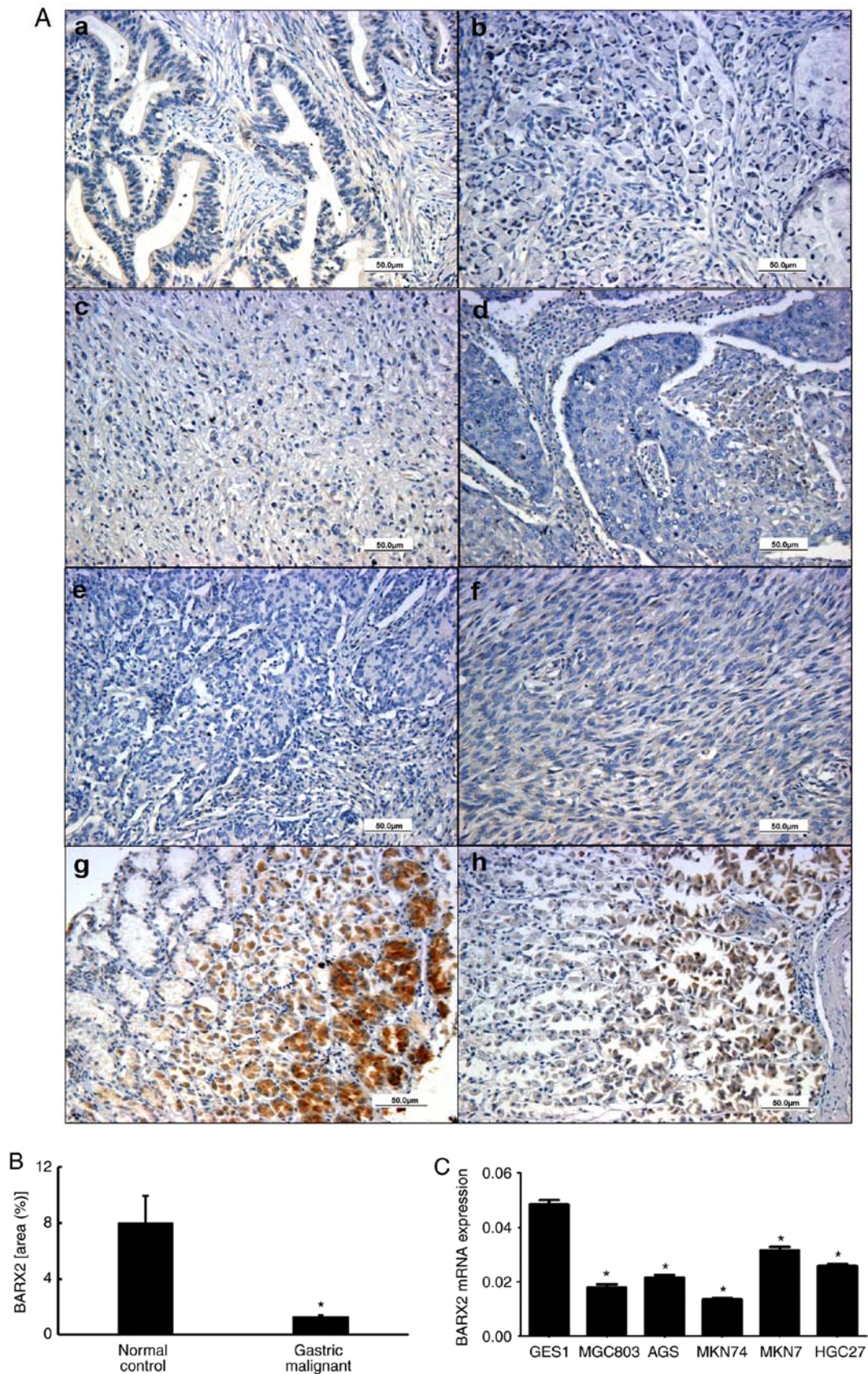


Figure 1. *BARX2* expression in normal and GC tissues. *BARX2* protein expression was weak and even absent in gastric malignant samples, including adenocarcinoma (T2N0M0) (Aa), signet-ring cell carcinoma (T2N0M0) (Ab), undifferentiated carcinoma (T2N0M0) (Ac), squamous cell carcinoma (T2N0M0) (Ad), carcinoid (T2N0M0) (Ae) and malignant interstitialoma (T2N0M0) (Af). *BARX2* stained as a yellowish brown and was commonly expressed in the cytoplasm and nucleus of the glandular epithelial cells in normal gastric mucosa (Ag and Ah), especially in the proliferative glandular lumens (Ah) as detected by immunohistochemistry. (B) Quantitative analysis shows that the positive staining area of *BARX2* was lower in the gastric malignant group (n=208, right bar), compared to normal controls (n=8, left bar, \*P<0.001). (C) qPCR analysis showed that *BARX2* mRNA levels were decreased and even lost in the gastric carcinoma cell lines MGC803, AGS, MKN74, MKN7, and HGC27, compared with the gastric mucosal cell line GES1 (P<0.001). Glyceraldehyde-3-phosphate dehydrogenase (GAPDH) was used as the internal control. The Student's t-test was used for statistical analysis. *BARX2*, BarH-like homeobox 2; GC, gastric cancer.

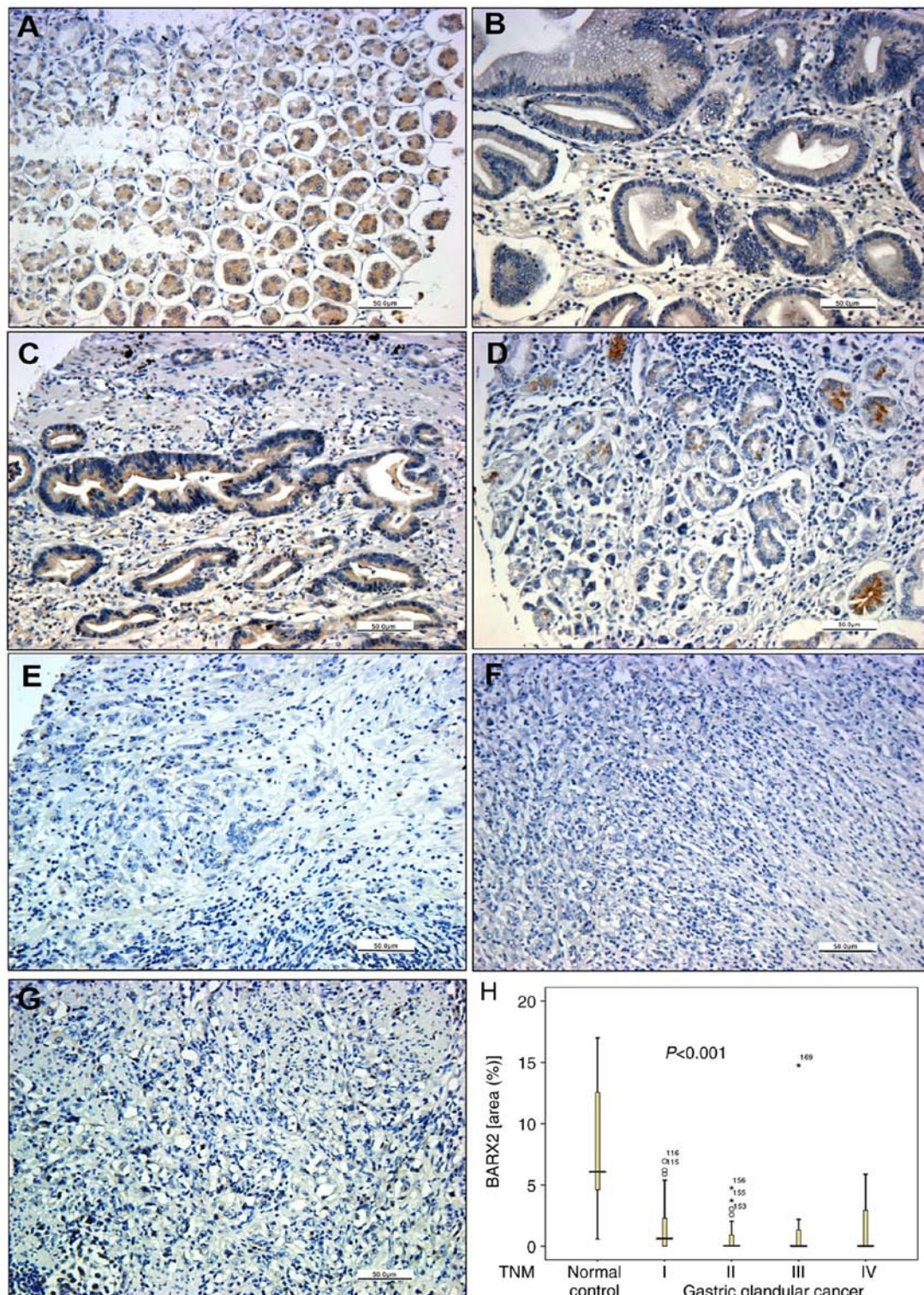


Figure 2. BARX2 expression in normal gastric mucosa and at various pathological stages of gastric adenocarcinoma. (A-G) Representative immunohistochemical staining images of BARX2 expression in normal gastric mucosa (A) and at various pathological stages of gastric adenocarcinoma: T1N0M0 (Ia) (B), T2N0M0 (Ib) (C), T3N0M0 (II) (D), T3N1M0 (IIIa) (E), T4N1M0 (IIIb) (F) and T4N3M1 (IV) (G). (H) BARX2 expression was progressively decreased from TNM stage I to IV in the gastric adenocarcinoma tissues ( $P < 0.001$ ). The Mann-Whitney U-test was used for statistical analysis. BARX2, BarH-like homeobox 2.

Overexpression of BARX2 is associated with suppression of GC cell proliferation, colony formation, and migration. Stable LV-BARX2 transfectants and LV-empty controls were established in AGS cells to observe the effects on the biological properties of GC cells *in vitro*. Three BARX2-overexpressing single clones detected by qPCR were selected and named

AGS-BARX2.3, AGS-BARX2.5 and AGS-BARX2.6 (Fig. S1). A polyclonal transfectant of AGS-BARX2 had higher expression of BARX2 compared to the AGS-LV cells (Fig. S1). The CCK-8 assay showed that the proliferation of AGS cells transfected with LV-BARX2 was significantly decreased at 48, 72, and 96 h with either  $2.0 \times 10^3$  cells ( $P < 0.01$ , Fig. 5A) or

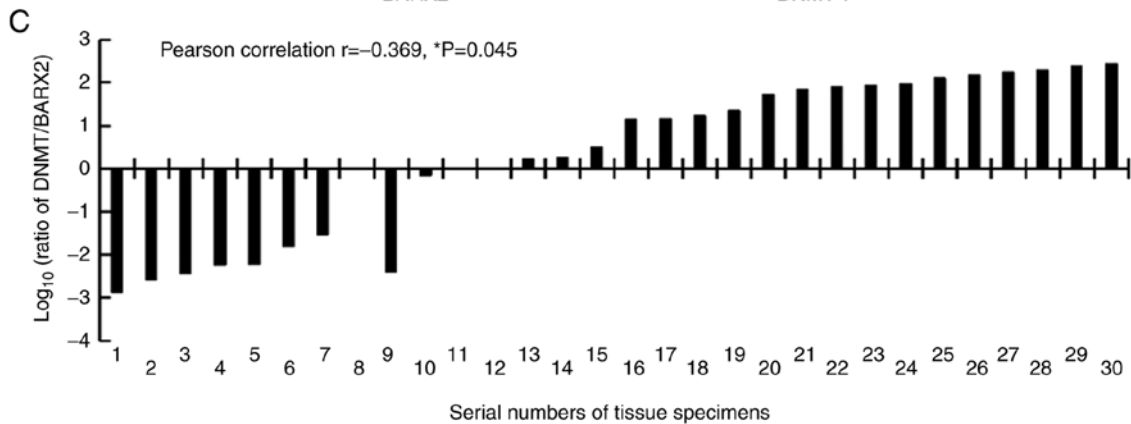
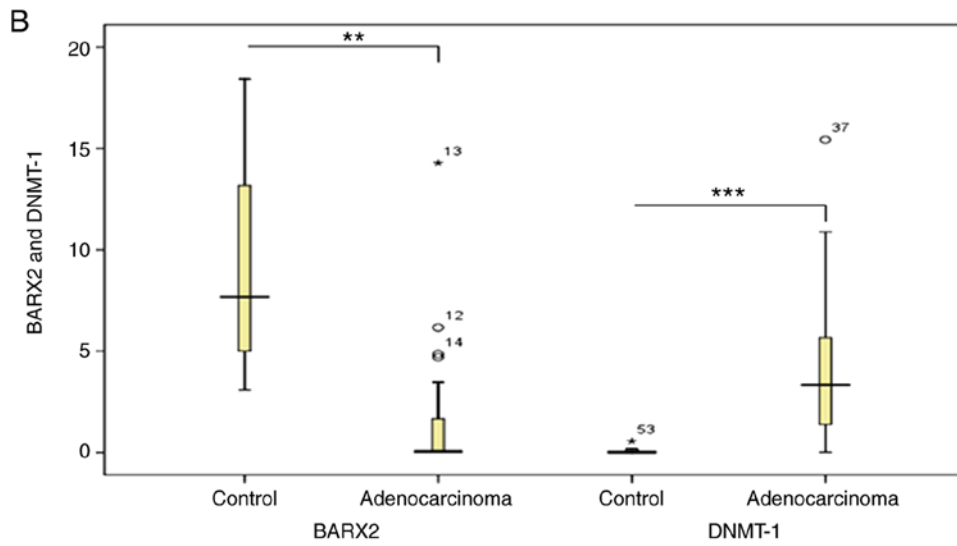
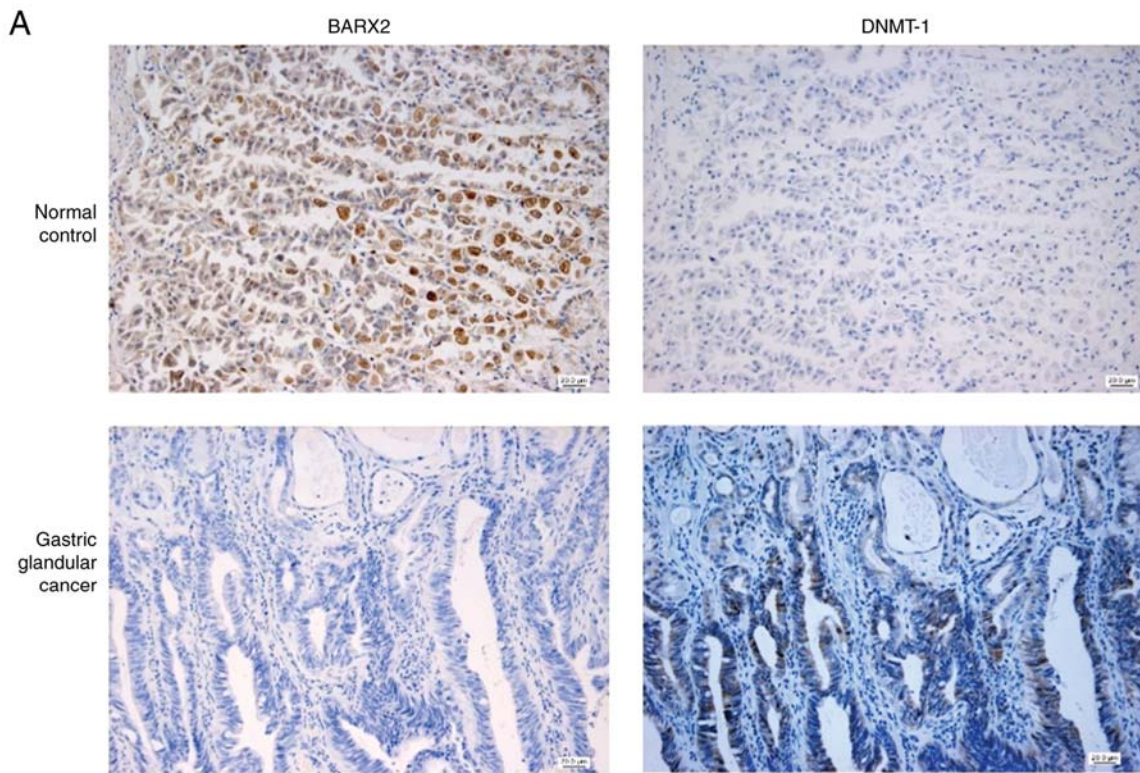


Figure 3. BARX2 and DNMT-1 expression in normal gastric mucosa and gastric adenocarcinoma. (A) Representative immunohistochemical staining images of BARX2 and DNMT-1 in normal gastric mucosa and gastric adenocarcinoma. (B) Compared with the normal mucosa, BARX2 expression was decreased and DNMT-1 expression was increased in gastric adenocarcinoma. \*\*P<0.01, \*\*\*P<0.001, compared with the normal mucosa. (C) BARX2 expression is negatively inversely correlated with DNMT expression. \*P<0.05. The Mann-Whitney U-test was utilized in B and Pearson correlation was used in C. The numbers 1-30 indicate the serial numbers of the tissue specimens. BARX2, BarH-like homeobox 2; DNMT-1, DNA methyltransferase 1.

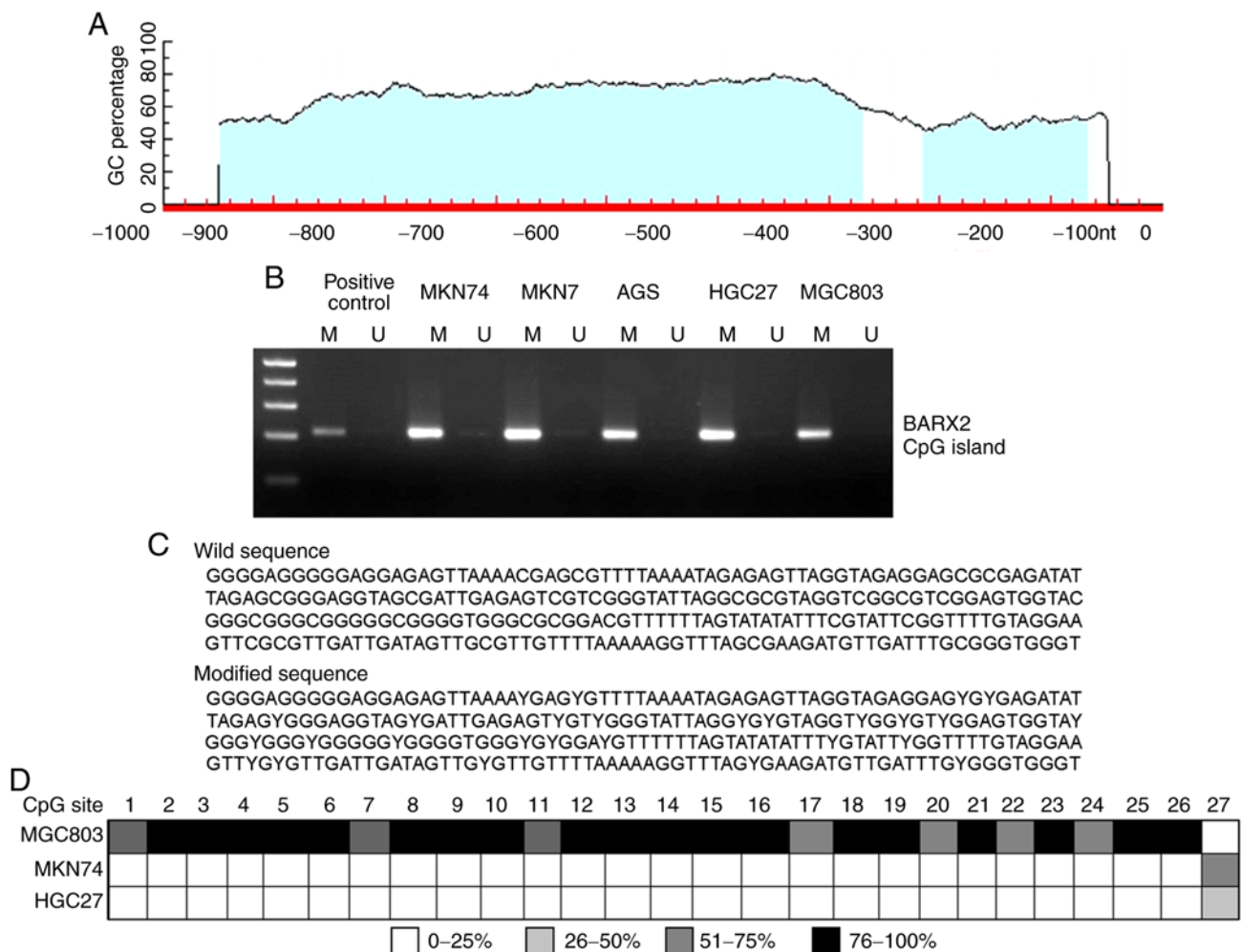


Figure 4. DNA methylation of the *BARX2* promoter was identified in GC cells. (A) Schematic diagram of putative CpG islands within the *BARX2* promoter identified as determined using bioinformatics analysis. (B) Putative CpG islands in five GC cell lines, as detected using methylation-specific polymerase chain reaction (MSP). M, methylated; U, unmethylated. (C) Methylation status of CpG sites within the functional promoter fragment, as detected using bisulfite DNA sequencing PCR analysis (BSP). The methylated CpG dinucleotides that could not be altered by bisulfite modification are replaced by letter Y. (D) Methylation status of the 27 CpG dinucleotides within the *BARX2* promoter fragment in three GC cell lines, including MGC803, MKN74, and HGC27, as detected using BSP. DNA hypermethylation was mostly observed in MGC803 cells. *BARX2*, BarH-like homeobox 2; GC, gastric cancer.

$4.0 \times 10^3$  cells ( $P < 0.001$ , Fig. 5B) seeded per well. The EdU assay also showed that ectopic expression of *BARX2* suppressed cell proliferation (Fig. 5C). There were fewer proliferating cells in the AGS-*BARX2* cells when compared to that of the AGS-LV cells. AGS-*BARX2* transfectants lost colony-forming capacity by nearly 40% compared to the AGS-LV controls cells; the percentages of colonies formed by AGS-*BARX2* and AGS-LV cells were  $27.37 \pm 1.65$  and  $45.57 \pm 1.29\%$ , respectively ( $P < 0.001$ , Fig. 5D and E). The migration ability of the AGS-*BARX2* cells was significantly lower compared to the AGS-LV cells (A460 value  $0.106 \pm 0.001$  vs.  $0.131 \pm 0.001$ ,  $P < 0.001$ , Fig. 5F and G). These observations indicate that overexpression of *BARX2* in GC cells is associated with suppression of cell proliferation, colony formation, and migration.

*Overexpression of BARX2 inhibits the tumorigenesis of GC cells in vivo.* Western blot analysis confirmed the overexpression of *BARX2* in the two stable transfectants (Fig. S1). Tumors formed in all 5 nude mice inoculated with AGS-LV cells and in 4 mice inoculated with AGS-*BARX2* cells 4 weeks after inoculation (Fig. 6A and B). The tumors from mice inoculated

with AGS-*BARX2* cells were significantly smaller compared to tumors from mice inoculated with AGS-LV cells 4 weeks after inoculation ( $48.17 \pm 14.93$  vs.  $100.83 \pm 5.29$  mm<sup>3</sup>,  $P = 0.011$ , Fig. 6C). In mice inoculated with AGS-*BARX2* cells, the tumors expressed higher levels of *BARX2* compared to mice inoculated with AGS-LV cells ( $P = 0.032$ ) (Fig. 6D and E). Additionally, the expression of Ki-67, PCNA, MMP3, MMP7, and MMP9 was decreased, while E-cadherin expression was increased in tumors formed by AGS-*BARX2* cells compared to expression in those formed by AGS-LV cells (Fig. 6D and E).

## Discussion

In the present study, BarH-like homeobox 2 (*BARX2*) expression was lower in gastric malignant tissues, especially gastric adenocarcinomas, compared to that noted in the normal gastric mucosa. The aberrant pattern of *BARX2* expression was accompanied by gradual aggravation of pathological stage and tissue differentiation. We found a negative correlation between *BARX2* and DNA methyltransferase 1 (DNMT-1) (a key marker of DNA methylation) expression and DNA methylation

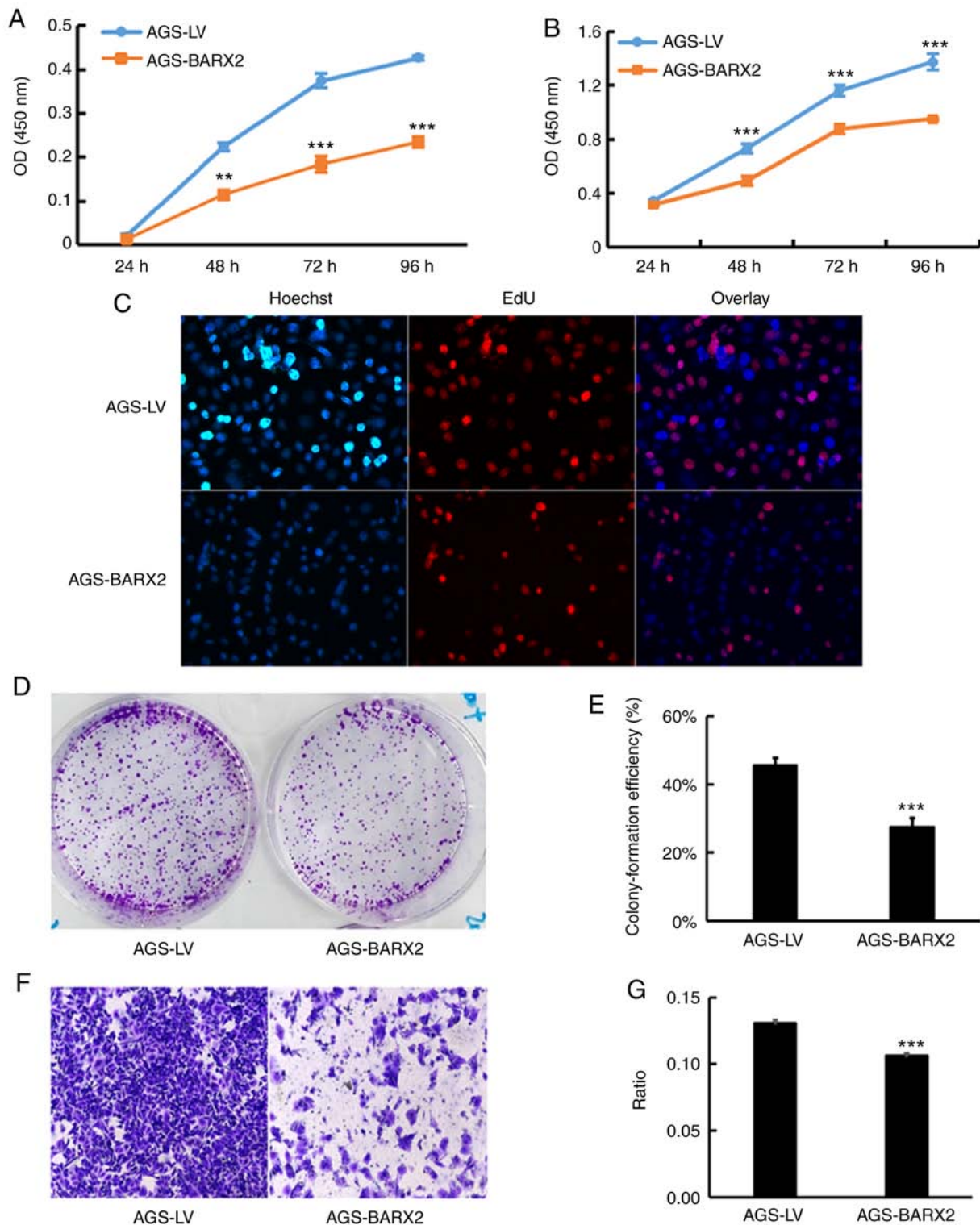


Figure 5. Overexpression of *BARX2* suppresses GC cell proliferation, colony formation, and migration. (A-C) Proliferation of AGS-BARX2 and AGS-LV cells, as assessed using CCK-8 (A and B) and 5'-ethynyl-2'-deoxyuridine (EdU) assays (C). Growth of AGS-BARX2 cells seeded at  $2.0 \times 10^3$  (A) or  $4.0 \times 10^3$  (B) were inhibited as evidenced by a lower proliferation index compared to AGS-LV cells. (D and E) Polyclonal transfectants ( $1.0 \times 10^3$ ) were seeded and cultured for 4 weeks. Colonies formed from the transfectants AGS-LV and AGS-BARX2 are shown and quantified. (F and G) Polyclonal transfectants ( $3 \times 10^4$ ) suspended in serum-free medium were seeded into the top compartment of Transwell culture inserts. The migration ratio of AGS-BARX2 cells was decreased significantly compared to the AGS-LV cells. \*\* $P < 0.01$  and \*\*\* $P < 0.001$ , compared with AGS-LV. The Student's t-test was used for statistical analysis. *BARX2*, BarH-like homeobox 2; GC, gastric cancer; EdU, 5'-ethynyl-2'-deoxyuridine.

in the promoter region of *BARX2*. Further *in vivo* experiments demonstrated that *BARX2* suppressed xenograft tumor formation and inhibited tumor cell proliferation and invasion in nude mice. Overexpression of *BARX2* inhibited gastric cancer (GC)

cell proliferation, invasion, and migration *in vitro* and xenograft tumor formation in nude mice. These findings indicate that *BARX2* could be a novel tumor suppressor that may play an important role in gastric carcinogenesis.

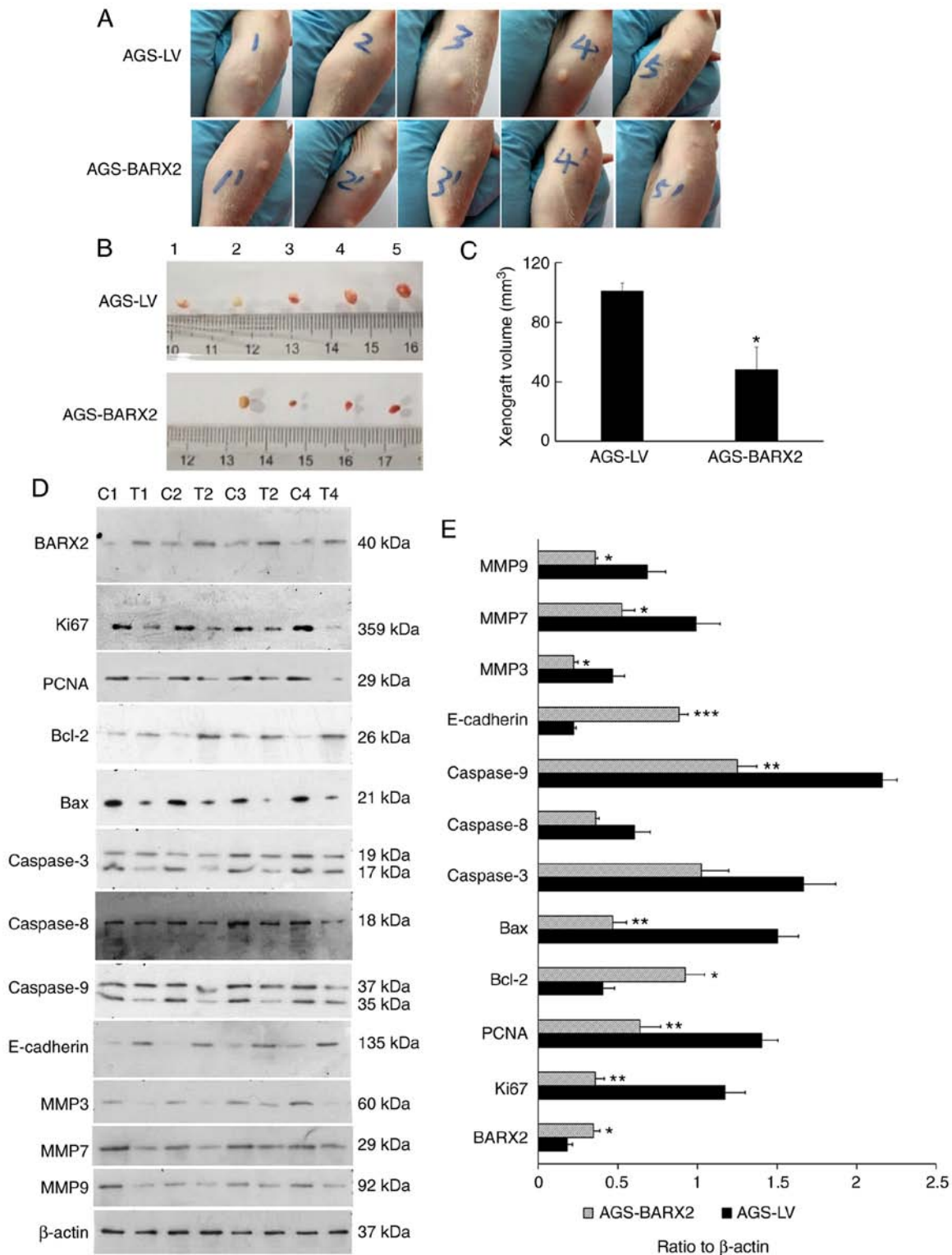


Figure 6. Overexpression of *BARX2* inhibits *in vivo* tumorigenesis. (A) BALB/c-nu/nu mice were inoculated subcutaneously with AGS-BARX2 and AGS-LV mono-colony transfectants ( $1.0 \times 10^7$ ) for 4 weeks. (B and C) Xenograft volume was calculated after euthanization of the mice. The numbers 1-5 indicate the serial numbers of nude mice in both groups inoculated with AGS-LV cells or AGS-BARX2 cells. Compared to the nude mice inoculated with AGS-LV cells, the AGS-BARX2 cell-inoculated mice developed smaller transplanted tumors. (D and E) All xenografts were collected for western blot analysis. Upregulation of *BARX2* suppressed expression of Ki-67, PCNA and MMPs (MMP3, MMP7 and MMP9), while upregulation of *BARX2* stimulated the expression of E-cadherin in the tumor tissues. Upregulation of *BARX2* also stimulated the expression of Bcl-2 but suppressed the expression of Bax and caspase-9 in the tumor tissues. \* $P < 0.05$ , \*\* $P < 0.01$ , \*\*\* $P < 0.001$ , compared with AGS-LV. The Student's t-test was used for statistical analysis. C, xenografts inoculated with AGS-LV cells; T, xenografts inoculated with AGS-BARX2 cells. *BARX2*, BarH-like homeobox 2; PCNA, proliferating cell nuclear antigen; MMP, metalloproteinase.

Human *BARX2* shares 100% identity within the homeodomain murine *Barx2*, which has been shown to be strongly

expressed in the crypts of the intestine tract and in the outer cells of gut muscles in rats (30), but is downregulated in many

malignancies including GC, colorectal cancer (20), hepatocellular carcinoma (19), ovarian cancer (17), and non-small cell lung carcinoma (21). In the present study, we found reduced expression of *BARX2* in gastric malignant tissues using immunohistochemistry and in GC cell lines using RT-PCR. Decreased *BARX2* expression was also associated with pathological TNM stage and cell differentiation in GC tissues. Consistently, *BARX2* was not upregulated in the five GC cell lines studied. Our results support a previous study by Mi *et al* (16). However, we used GC tissue and analyzed *BARX2* expression using ImageJ, which has never been previously measured. Interestingly, *BARX2* mRNA levels were decreased in AGS, MKN74 and MKN7 cells and even absent in HGC72 and BGC803 cells. These findings indicate that *BARX2* is associated with cell differentiation and tumor prognosis as MKN74, MKN7, AGS, and BGC803 cells are all differentiated GC cell lines, whereas HGC27 is an undifferentiated gastric carcinoma.

The mechanisms by which *BARX2* is downregulated or lost remain to be elucidated. Mi *et al* reported that overexpression of *BARX2* reduced nuclear  $\beta$ -catenin but increased cytoplasmic  $\beta$ -catenin, suggesting that *BARX2* functions as a tumor suppressor in GC cells (16). However, the previous study did not further explore the molecular mechanism by which *BARX2* expression is inhibited. Epigenetic modification, such as DNA methylation, is known to play an important role in gene transcription (10). DNA methyltransferase (DNMT) is a key enzyme that regulates gene expression during DNA methylation modification, a process that occurs on some promoters of tumor-suppressor genes in GC (24). In the present study, we first found an inverse correlation between *BARX2* and DNMT-1 protein expression in GC tissues. In addition, methylation-specific PCR analysis (MSP) and bisulfite DNA sequencing PCR analysis (BSP) showed that DNA hypermethylation was present in the putative conserved promoter region of *BARX2* in GC cells. This suggests that DNA methylation modifications are involved in transcriptional regulation of the *BARX2* promoter, leading to silencing of *BARX2* in GC. However, how DNA methylation regulates *BARX2* transcription and if there are other epigenetic modifications require further research.

In the present study, we found that the xenograft volume was significantly decreased in the AGS-*BARX2* group compared to the AGS-LV control group. Both proliferation markers Ki-67 and PCNA were significantly downregulated, which was consistent with our *in vitro* experimental results. In addition, we found that *BARX2* overexpression was associated with changes in the expression of several apoptotic proteins, including upregulation of Bcl-2 and downregulation of Bax and caspase-9; however, there was no change in the expression of caspase 3. It is well known that the apoptosis process is complex, involving both exogenous and endogenous pathways (31,32). Although Bcl-2 and Bax play important roles in regulating apoptosis, they are not the decisive factors in the occurrence and development of apoptosis, which is primarily executed by caspase 3 (31,32). Thus, the findings in the present study suggest that overexpression of *BARX2* may regulate the expression of Bax and Bcl-2, but does not necessarily induce apoptosis. We speculate that *BARX2* overexpression inhibits the proliferation of GC cells and further induces a

compensatory response that alters expression of apoptotic proteins, but without substantial induction of apoptosis. More extensive investigation is required to further reveal the effect of *BARX2* on proliferation and apoptosis.

*BARX2* regulates proliferation, migration, invasion, and metastasis of tumor cells by altering cytoskeletal rearrangement, cell-matrix interaction, and extracellular matrix remodeling, all processes that are related to the Wnt/ $\beta$ -catenin signaling pathway. E-cadherin is a downstream target gene of the Wnt signaling pathway (33). *BARX2* interacts with Wnt to regulate proliferation and differentiation of embryonic myoblasts (34). Loss of *BARX2* is negatively associated with Ki-67 expression and epithelial-mesenchymal transition (EMT) markers, including E-cadherin and vimentin in HCC (19), similar to another Bar homeobox family genes (35). Recent studies have found that downregulation of *BARX2* in GC is related to  $\beta$ -catenin (16). Our present study supports the hypothesis that *BARX2* regulates proliferation,  $\beta$ -catenin expression, and metastasis of GC through the Wnt signaling pathway. Because *BARX2* is essentially a transcription factor, the downstream effectors of this protein need to be further identified in future studies. Stevens and Meech (18) found decreased expression of *BARX2* and its direct target, estrogen receptor- $\alpha$  (ESR), in breast cancer cells. *BARX2* upregulated the expression of MMP9 and metalloproteinase inhibitor 4 (TIMP4), which was in response to extracellular matrix (ECM) signals, and ultimately promoted invasion of breast cancer cells (18). Mi *et al* reported that overexpression of *BARX2* was associated with reduced expression of nuclear  $\beta$ -catenin, but increased expression of cytoplasmic  $\beta$ -catenin, and that enhanced *BARX2* expression reversed the inhibitory effect of the Wnt signaling pathway in GC (16). Chen *et al* (21) showed that *BARX2* decreased cell proliferation, migration, and aerobic glycolysis by inhibiting the Wnt/ $\beta$ -catenin signaling pathway in non-small cell lung carcinoma.

In the present study, we also explored the effect of *BARX2* on the biological functions of GC cells and the potential underlying molecular mechanisms. Our experiments showed that *BARX2* overexpression inhibited proliferation and invasion *in vitro* and suppressed the growth of transplanted tumors *in vivo*. Furthermore, *BARX2* overexpression was associated with altered expression of a series of molecular proteins. Specifically, *BARX2* overexpression downregulated Ki-67, PCNA, MMP3, MMP7, MMP9 and upregulated E-cadherin *in vivo*. Our findings suggest that the silencing of *BARX2* promotes gastric carcinogenesis by responding to ECM and Wnt signals and regulating genes that are involved in ECM remodeling and GC invasion. Our study supports some previous studies (16,17,19,21) in that *BARX2* suppressed proliferation, invasion, and migration of several cancer cell lines, but our data are not consistent with a previous study (18) that showed that *BARX2* promotes invasion of breast cancer cells by increasing MMP9 and TIMP4 in the presence of ESR. The discrepancies between these studies may be explained by the hypothesis that *BARX2* bidirectionally regulates carcinogenesis in different organs and tissues through various target factors, such as estrogen. Indeed, this bidirectional regulation has been reported for other homologous genes, such as *PDX1* (7,9). However, this hypothesis and the detailed mechanisms need to be further explored.

Despite the major exciting findings presented here, we were not able to fully explain the effects of the epigenetic modification on *BARX2* transcription and, more importantly, to determine the interactive effects between *BARX2* and the Wnt/ $\beta$ -catenin signaling pathway. We are currently planning to establish a GC transplantation model to explore the regulatory effects of *BARX2* on the Wnt/ $\beta$ -catenin pathway or vice versa, using techniques such as RNA-Seq and ChIP-Seq (36-39). In addition, our preliminary immunohistochemical experiments on the expression pattern of *BARX2* in colorectal cancer, surprisingly, indicate that *BARX2* protein expression is higher in colorectal cancer compared to normal colon mucosa (data not shown). This observation suggests that the function of *BARX2* in gastrointestinal tumors is complex and that *BARX2* may play different roles depending on the type of malignancy and tumor environment and condition. More extensive investigation is required to elucidate the roles of *BARX2*.

In conclusion, *BARX2* expression is aberrantly reduced in GC, which is associated with DNA methylation of its promoter. *BARX2* inhibits GC cell proliferation, migration, and tumor formation. Our findings suggest that *BARX2* could act as a tumor suppressor in gastric carcinogenesis and, more importantly, *BARX2* may be a potential target for GC treatment.

#### Acknowledgements

We thank Dr Harry H-X Xia for editing the manuscript.

#### Funding

The present study was supported by the Natural Science Foundation of Guangdong Province of China (2016A030313765), the Medical Scientific Research Foundation of Guangdong Province of China (A2017070 and A2017122), and the Project of Administration of Traditional Chinese Medicine of Guangdong Province of China (20191009).

#### Availability of data and materials

The datasets generated and analyzed during the present study are available from the corresponding author on reasonable request.

#### Authors' contributions

JM and ZSL conceived and designed the research study, and had primary responsibility for the final content. LLX and JM collected the data and conducted the research. XQY, LSX and WHS analyzed and interpreted the data. JM wrote the initial manuscript, and WHS revised the manuscript. SMZ and SL performed additional cell experiments according to the reviewers' suggestions. All authors read and approved the manuscript and agree to be accountable for all aspects of the research in ensuring that the accuracy or integrity of any part of the work are appropriately investigated and resolved.

#### Ethics approval and consent to participate

This study was approved by Guangdong General Hospital Ethics Committee. All procedures performed in studies

involving animals were in accordance with the ethical standards of the institution or practice at which the studies were conducted.

#### Patient consent for publication

Not applicable.

#### Competing interests

The authors declare that they have no competing interests.

#### References

- Torre LA, Bray F, Siegel RL, Ferlay J, Lortet-Tieulent J and Jemal A: Global cancer statistics, 2012. *CA Cancer J Clin* 65: 87-108, 2015.
- Siegel RL, Miller KD and Jemal A: Cancer statistics, 2016. *CA Cancer J Clin* 66: 7-30, 2016.
- Chen W, Zheng R, Baade PD, Zhang S, Zeng H, Bray F, Jemal A, Yu XQ and He J: Cancer statistics in China, 2015. *CA Cancer J Clin* 66: 115-132, 2016.
- He S, Del Viso F, Chen CY, Ikmi A, Kroesen AE and Gibson MC: An axial Hox code controls tissue segmentation and body patterning in *Nematostella vectensis*. *Science* 361: 1377-1380, 2018.
- Holland PW: Evolution of homeobox genes. *Wiley Interdiscip Rev Dev Biol* 2: 31-45, 2013.
- Stoffers DA, Heller RS, Miller CP and Habener JF: Developmental expression of the homeodomain protein IDX-1 in mice transgenic for an IDX-1 promoter/lacZ transcriptional reporter. *Endocrinology* 140: 5374-5381, 1999.
- Ma J, Chen M, Wang J, Xia HH, Zhu S, Liang Y, Gu Q, Qiao L, Dai Y, Zou B, *et al*: Pancreatic duodenal homeobox-1 (PDX1) functions as a tumor suppressor in gastric cancer. *Carcinogenesis* 29: 1327-1333, 2008.
- Guz Y, Montminy MR, Stein R, Leonard J, Gamer LW, Wright CV and Teitelman G: Expression of murine STF-1, a putative insulin gene transcription factor, in beta cells of pancreas, duodenal epithelium and pancreatic exocrine and endocrine progenitors during ontogeny. *Development* 121: 11-18, 1995.
- Liu T, Gou SM, Wang CY, Wu HS, Xiong JX and Zhou F: Pancreas duodenal homeobox-1 expression and significance in pancreatic cancer. *World J Gastroenterol* 13: 2615-2618, 2007.
- Herring BP, Kriegel AM and Hoggatt AM: Identification of Barx2b, a serum response factor-associated homeodomain protein. *J Biol Chem* 276: 14482-14489, 2001.
- Naka T and Yokose S: Immunohistochemical localization of barx2 in the developing fetal mouse submandibular glands. *Acta Histochem Cytochem* 42: 47-53, 2009.
- Meech R, Edelman DB, Jones FS and Makarenkova HP: The homeobox transcription factor Barx2 regulates chondrogenesis during limb development. *Development* 132: 2135-2146, 2005.
- Olson LE, Zhang J, Taylor H, Rose DW and Rosenfeld MG: Barx2 functions through distinct corepressor classes to regulate hair follicle remodeling. *Proc Natl Acad Sci USA* 102: 3708-3713, 2005.
- Jones FS, Kiuoussi C, Copertino DW, Kallunki P, Holst BD and Edelman GM: Barx2, a new homeobox gene of the Bar class, is expressed in neural and craniofacial structures during development. *Proc Natl Acad Sci USA* 94: 2632-2637, 1997.
- Stevens TA, Iacovoni JS, Edelman DB and Meech R: Identification of novel binding elements and gene targets for the homeodomain protein BARX2. *J Biol Chem* 279: 14520-14530, 2004.
- Mi Y, Zhao S, Zhou C, Weng J, Li J, Wang Z, Sun H, Tang H, Zhang X, Sun X, *et al*: Downregulation of homeobox gene Barx2 increases gastric cancer proliferation and metastasis and predicts poor patient outcomes. *Oncotarget* 7: 60593-60608, 2016.
- Sellar GC, Li L, Watt KP, Nelkin BD, Rabiasz GJ, Stronach EA, Miller EP, Porteous DJ, Smyth JF and Gabra H: BARX2 induces cadherin 6 expression and is a functional suppressor of ovarian cancer progression. *Cancer Res* 61: 6977-6981, 2001.
- Stevens TA and Meech R: BARX2 and estrogen receptor-alpha (ESR1) coordinately regulate the production of alternatively spliced ESR1 isoforms and control breast cancer cell growth and invasion. *Oncogene* 25: 5426-5435, 2006.

19. Zhang Y, Zhang JX, Huang LL, He LJ, Liao YJ, Lai YR, Deng HX, Tian XP, Kung HF, Xie D and Zhu SL: Low expression of *BARX2* in human primary hepatocellular carcinoma correlates with metastasis and predicts poor prognosis. *Hepatol Res* 45: 228-237, 2015.
20. Mi Y, Zhao S, Zhang W, Zhang D, Weng J, Huang K, Sun H, Tang H, Zhang X, Sun X, *et al*: Down-regulation of *Barx2* predicts poor survival in colorectal cancer. *Biochem Biophys Res Commun* 478: 67-73, 2016.
21. Chen H, Zhang M, Zhang W, Li Y, Zhu J, Zhang X, Zhao L, Zhu S and Chen B: Downregulation of BarH-like homeobox 2 promotes cell proliferation, migration and aerobic glycolysis through Wnt/ $\beta$ -catenin signaling, and predicts a poor prognosis in non-small cell lung carcinoma. *Thorac Cancer* 9: 390-399, 2018.
22. Wong NA, Britton MP, Choi GS, Stanton TK, Bicknell DC, Wilding JL and Bodmer WF: Loss of *CDX1* expression in colorectal carcinoma: Promoter methylation, mutation, and loss of heterozygosity analyses of 37 cell lines. *Proc Natl Acad Sci USA* 101: 574-579, 2004.
23. Guo M, House MG, Suzuki H, Ye Y, Brock MV, Lu F, Liu Z, Rustgi AK and Herman JG: Epigenetic silencing of *CDX2* is a feature of squamous esophageal cancer. *Int J Cancer* 121: 1219-1226, 2007.
24. Ma J, Wang JD, Zhang WJ, Zou B, Chen WJ, Lam CS, Chen MH, Pang R, Tan VP, Hung IF, *et al*: Promoter hypermethylation and histone hypoacetylation contribute to pancreatic-duodenal homeobox 1 silencing in gastric cancer. *Carcinogenesis* 31: 1552-1560, 2010.
25. Ushijima T: Detection and interpretation of altered methylation patterns in cancer cells. *Nat Rev Cancer* 5: 223-231, 2005.
26. Esteller M: Cancer epigenomics: DNA methylomes and histone-modification maps. *Nat Rev Genet* 8: 286-298, 2007.
27. Livak KJ and Schmittgen TD: Analysis of relative gene expression data using real-time quantitative PCR and the  $2^{-\Delta\Delta C(T)}$  method. *Methods* 25: 402-408, 2001.
28. Zhao F, Xuan Z, Liu L and Zhang MQ: TRED: A transcriptional regulatory element database and a platform for in silico gene regulation studies. *Nucleic Acids Res* 33 (Suppl): D103-D107, 2005.
29. Li LC and Dahiya R: MethPrimer: Designing primers for methylation PCRs. *Bioinformatics* 18: 1427-1431, 2002.
30. Sander GR and Powell BC: Expression of the homeobox gene *barx2* in the gut. *J Histochem Cytochem* 52: 541-544, 2004.
31. Verbrugge I, Johnstone RW and Smyth MJ: SnapShot: Extrinsic apoptosis pathways. *Cell* 143: 1192-1192.e2, 1192.e1-1192.e2, 2010.
32. Green DR and Llambi F: Cell death signaling. *Cold Spring Harb Perspect Biol* 7: 7, 2015.
33. Chiurillo MA: Role of the Wnt/ $\beta$ -catenin pathway in gastric cancer: An in-depth literature review. *World J Exp Med* 5: 84-102, 2015.
34. Zhuang L, Hulin JA, Gromova A, Tran Nguyen TD, Yu RT, Liddle C, Downes M, Evans RM, Makarenkova HP and Meech R: *Barx2* and *Pax7* have antagonistic functions in regulation of wnt signaling and satellite cell differentiation. *Stem Cells* 32: 1661-1673, 2014.
35. Wang G, Liu J, Cai Y, Chen J, Xie W, Kong X, Huang W, Guo H, Zhao X, Lu Y, *et al*: Loss of *Barx1* promotes hepatocellular carcinoma metastasis through up-regulating *MGAT5* and *MMP9* expression and indicates poor prognosis. *Oncotarget* 8: 71867-71880, 2017.
36. Chen C, Lu Y, Liu J, Li L, Zhao N and Lin B: Genome-wide ChIP-seq analysis of *TCF4* binding regions in colorectal cancer cells. *Int J Clin Exp Med* 7: 4253-4259, 2014.
37. Debebe A, Medina V, Chen CY, Mahajan IM, Jia C, Fu D, He L, Zeng N, Stiles BW, Chen CL, *et al*: Wnt/ $\beta$ -catenin activation and macrophage induction during liver cancer development following steatosis. *Oncogene* 36: 6020-6029, 2017.
38. Sarkar A, Huebner AJ, Sulahian R, Anselmo A, Xu X, Flattery K, Desai N, Sebastian C, Yram MA, Arnold K, *et al*: *Sox2* suppresses gastric tumorigenesis in mice. *Cell Rep* 16: 1929-1941, 2016.
39. Laurent A, Calabrese M, Warnatz HJ, Yaspo ML, Tkachuk V, Torres M, Blasi F and Penkov D: ChIP-Seq and RNA-Seq analyses identify components of the Wnt and Fgf signaling pathways as *Prepl* target genes in mouse embryonic stem cells. *PLoS One* 10: e0122518, 2015.



This work is licensed under a Creative Commons Attribution-NonCommercial-NoDerivatives 4.0 International (CC BY-NC-ND 4.0) License.